Optimal Melting Interface Tracking in Laser-Aided Powder Deposition Processes

Xiaoqing Cao and Beshah Ayalew

International Center for Automotive Research, Clemson University, Greenville, SC 29607

REVIEWED

Abstract

This paper presents a systematic control inputs optimization method for melting interface tracking in laser-aided powder deposition (LAPD) processes. Using a proposed interface approximation and a coordinate system moving with the laser source, and adopting the enhanced thermal conductivity method, the process model is first reduced to a set of coupled partial differential equations (PDEs) in fixed spatial domains. Then, the control problem of achieving process target properties is formulated as one of optimizing the control inputs to track a prescribed melting interface which is approximated from required process target parameters. This proposed optimization scheme is solved by the adjoint-based gradient method for which an algorithm is provided. A weighting scheme is also proposed to overcome feasibility issues with poor interface specifications and still achieve improved tracking of target parameters. The proposed scheme is illustrated through a simulation-based case study on a laser cladding process.

Introduction

Laser-aided powder deposition (LAPD) processes employ directed laser power for material processing and part manufacturing. Example processes include: laser cladding, laser sintering, laser metal deposition (LMD), digital direct manufacturing (DDM), etc. Due to the existence of multiple phenomena such as heat transfer with phase change on the substrate, thermo-capillary induced fluid flow in the melting pool [1], free surface formation [2-4] as well as laser-powder interaction [5], models of these processes often involve coupled nonlinear partial differential equations (PDEs) in space and time [2, 6-8]. While such PDE-based models offer accurate and explicit representation of the spatio-temporal physical interactions, their high computational burden often limits their use for practical control design and implementation. By introducing the enhanced thermal conductivity method [9, 10], the influence of fluid flow to melting pool formation is implicitly considered. This results in a reduced system model similar to that in the so-called two-phase Stefan problem [11-13], which describes heat transfer with phase change.

One of the essential considerations in control of the Stefan problem is the motion of the melting interface (interface between solid and liquid domains). This consideration is also found in LAPD processes since important process properties such as the powder deposition efficiency (the portion of powder particles that fall into the melting pool range) and the penetration depth (metallurgical bond) on the substrate are implied in the geometric shape of this interface. Thus, it is of great importance to control the geometric shape of melting interface in LAPD processes.

For the classic two-phase Stefan problem, optimal control is reported to be an effective strategy for regulating the geometry of the melting interface. This is often achieved by

formulating it as a control input optimization problem with PDE constraints [11-13]. Similar control strategies can be found in a laser cutting process [14, 15]. In [16], an optimal control scheme was proposed for a laser welding process where only the laser power distribution on the substrate was optimized.

In this paper, we focus on the intermediate segments of LAPD processes where steady state can be assumed, and determine the (open-loop) optimal control inputs (laser power and scanning speed) to achieve pre-specified process target properties. By introducing an interface approximating method and a coordinate system moving with the laser source, the free interfaces, mainly the melting (solid-liquid) interface, are approximated directly from the desired process target parameters (those related to powder catch efficiency, deposition height and penetration depth, etc.). Then, we reformulate the process control problem as one of tracking the melting interface as close to the desired (approximated) one as possible with the optimal control inputs. This view allows us to formulate and solve the PDE-constrained optimization problem with the adjoint-based gradient method. A weighting function is also proposed under this optimization scheme to overcome the possible lack of physical feasibility of the approximated interface.

The rest of the paper is organized as follows: Section 2 discusses the adopted process model and the practical interface approximations proposed in this paper. Section 3 details the formulation of the optimal melting interface tracking problem and the solution of the resulting control inputs optimization problem. The derived adjoint PDE equations as well as the computational algorithm for obtaining the optimal solution are also included. Section 4 provides a case study on the laser cladding process. Conclusions are included in Section 5.

Modeling of LAPD Processes

Process Overview

The physical essences of LAPD processes can be illustrated in Fig. 1. A laser beam with high power density sweeps on the surface of the substrate, creating a melting pool. The powder material is either pre-placed on the substrate or injected into the melting pool by coaxial or lateral powder nozzles. After the melting and solidification processes, a metallurgical bond is formed between the deposited layer and the substrate material.

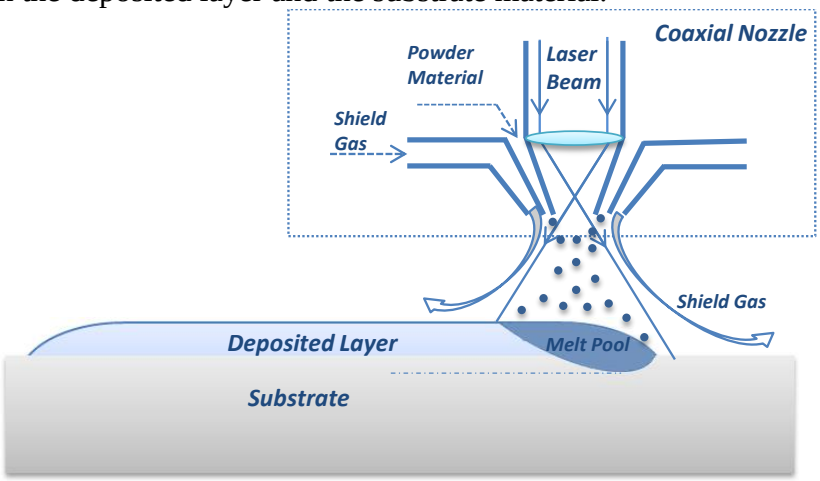

Fig. 1 Schematic of LAPD processes

The mathematical model of LAPD processes is outlined in Fig. 2. It is a two-dimensional (2D) steady-state model for the coaxial powder nozzle configuration. The coordinate system is selected to move at the same constant speed as the laser source while the origin is fixed at the nozzle position on the substrate surface. The computational domain contains the solid phase Ω_S and the liquid phase Ω_L, which share the melting interface Γ_{SL}. Although it is not listed as a computational domain, the gas phase does exist as the ambient and shares interfaces with the solid and liquid phases, which are denoted as Γ_{SG} and Γ_{LG}, respectively. The remaining boundary of the solid is denoted by Γ_S. The layer height and the melting pool depth are denoted by H and D, respectively.

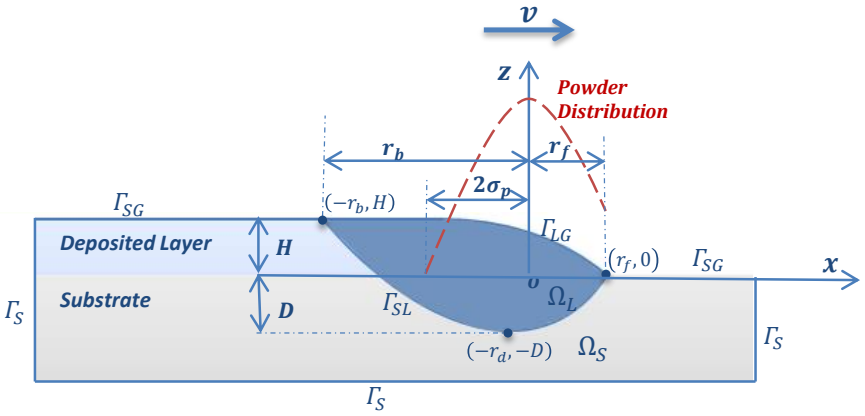

Fig. 2 Mathematical model of the process

Models for Interface Approximations

One of the most challenging aspects in modeling and control of LAPD processes is the existence of free boundaries between multiple phases, more specifically, the melting and liquid-gas interfaces. As mentioned in the introduction, we offer a practical method for approximating these interfaces in order to make the optimization problem tractable. To motivate the idea, we use the schematic in Fig. 2 and make the observation that, in steady state, the geometric parameters, which include front/back radius (r_f/r_b), deposition height H, and melting pool depth D, relate directly to the critical target process properties such as powder deposition efficiency and penetration depth on the substrate. Thus, by pre-specifying these geometric parameters from the requirements of process properties, the geometry of the target interfaces can be constructed approximately. This, along with the choice of the coordinate system moving with the laser source (and powder nozzle), reduces the modeling domains into two fixed domains Ω_S and Ω_L.

In this paper, based on the geometric relationship implied in Fig. 2, the profile of the liquid-gas interface can be approximated to be parabolic as follows, similar to the proposal in [17]:

$$f_{LG}(x) = \begin{cases} H\left[1 - \left(\dfrac{x + 2\sigma_P}{r_f + 2\sigma_P}\right)^2\right], & x \in [-2\sigma_P, r_f] \\ H, & x \in [-r_b, -2\sigma_P] \end{cases} \quad (1)$$

where the relationship between r_f, r_b and σ_P is selected to be $r_f < 2\sigma_P < r_b$ and $2\sigma_P$ denotes the powder extinction range on the substrate. This assumes that the powder particles would only be deposited within the melting pool and considers the trade-off between the delivery efficiency and deposition rate of the powder material [18].

In a similar manner, the melting interface can also be approximated by the following double-parabolic equation:

$$f_{SL}(x) = \begin{cases} (H + D)\left(\frac{x + r_d}{r_b - r_d}\right)^2 - D, & x \in [-r_b, -r_d] \\ D\left(\frac{x + r_d}{r_f + r_d}\right)^2 - D, & x \in [-r_d, r_f] \end{cases} \quad (2)$$

where r_d is the position of melting pool depth in the laser moving direction.

Having approximated the desired geometry of the two interphase boundaries in terms of the desired process target parameters, we then use them as the target fixed boundaries (in the moving frame) for the domains of the liquid and solid phases. This significantly simplifies the underlying model and the control based on this model.

Heat Transfer Model

In this paper, we restrict ourselves to the modeling and control of steady-state LAPD processes in the moving coordinate system. This can be justified from the fact that when the laser beam moves at a constant speed along the substrate surface, critical system properties such as the temperature distribution, the position of melting interface as well as the geometry of melting pool maintain the same. Thus, it is reasonable to assume a steady-state process model in the coordinate system that moves at the same speed as the laser source and use this model for subsequent control inputs optimization. Transient sections and disturbance handling can be accommodated with suitable feedback control [17, 19, 20] and will not be treated in this work. Also, as already stated in the introduction, we shall adopt an anisotropic enhanced thermal conductivity approach for the liquid phase to retain fluid flow effects in the mathematical model described as follows:

$$-\rho_S C_S v \cdot \nabla T_S = k_S \Delta T_S \quad \text{in } \Omega_S \quad (3.1)$$
$$-\rho_L C_L v \cdot \nabla T_L = k_L^* \Delta T_L \quad \text{in } \Omega_L \quad (3.2)$$
$$k_S \frac{\partial T_S}{\partial \mathbf{n}} = \alpha_{att}(x) * u \quad \text{on } \Gamma_{SG} \quad (3.3)$$
$$k_L^* \frac{\partial T_L}{\partial \mathbf{n}} = \alpha_{att}(x) * u \quad \text{on } \Gamma_{LG} \quad (3.4)$$
$$T_S = T_a \quad \text{on } \Gamma_S \quad (3.5)$$
$$T_L = T_S \quad \text{on } \Gamma_{SL} \quad (3.6)$$
$$\rho_S L v \cdot \mathbf{n} = \left[k \frac{\partial T}{\partial \mathbf{n}}\right]_L^S \quad \text{on } \Gamma_{SL} \quad (3.7)$$

where $k_L^* = \alpha * k_L$ is the enhanced thermal conductivity with an enhancement factor α applied in the liquid domain. **n** is the outward unit vector normal to the boundary surface. The expression $\left[k\frac{\partial T}{\partial \mathbf{n}}\right]_L^S$ represents the heat flux jump across the melting interface due to phase change [16]. L is the latent heat of fusion, u is the laser power and v is the scanning speed. $\alpha_{att}(x)$ is the laser power attenuation coefficient [21].

The LHS in the first two equations denotes the heat convection in the moving coordinate in both the solid and liquid domains. On the top surface of the substrate, heat transfer is dominated by laser irradiation, which is modeled by Neumann boundary condition. For the solid boundary Γ_S, since the substrate is usually large enough compared with the melting pool, a Dirichlet boundary condition of a constant ambient temperature is applied. On the melting interface, the temperature is constrained by the condition of temperature continuity. The heat flux discontinuity induced by the latent heat of fusion, which is also known as the Stefan condition, is explicitly addressed by the last equation.

Optimal Melting Interface Tracking

In this section, the optimal melting interface tracking problem is first formulated explicitly as a multivariable control input optimization problem. Then, the derived adjoint equations and the computational algorithm for solving the optimization problem are outlined briefly.

Problem Formulation

The main control objective of LAPD processes is to achieve desired process properties in terms of deposition height, powder delivery efficiency as well as the penetration depth, etc. A set of related process target parameters can be specified to reflect these desired properties. In this paper, these process target parameters are selected to be the back/front radius r_b/r_f, deposition height H, penetration depth D and its position r_d (see Fig. 2).

As pointed out above, by introducing the interface approximations, the problem can be transformed into a melting interface tracking problem. To be more specific, by designing a desired and fixed melting interface geometry, which is specified using the process target parameters, the optimization objective can be set to minimize the difference between the temperature on this specified melting interface and the melting temperature of the substrate via an optimal combination of control inputs, namely the laser power u and scanning speed v. This can be formulated mathematically as follows:

$$\mathrm{Min}_{u,v}\ J(T,u,v) = \frac{\alpha_1}{2}\int_{\Gamma_{SL}} w(x)\left(\frac{T-T_m}{T_m}\right)^2 dl \tag{4.1}$$

$$\text{Subject to:}\quad T = Sys(u,v) \tag{4.2}$$

where T_m is the substrate melting temperature, α_1 is a normalization constant and the constraint in Eq. (4.2) represents the system PDEs listed in Eq. (3) compactly. $w(x)$ is a weighting function that is parameterized as:

$$w(x) = 1 + \alpha_2 e^{-\left(\frac{x+r_b}{\sigma_2}\right)^2} + \alpha_3 e^{-\left(\frac{x-r_f}{\sigma_3}\right)^2} + \alpha_4 e^{-\left(\frac{x+r_d}{\sigma_4}\right)^2} \quad (5)$$

where the variables α_i, σ_i $(i = 2, 3, 4)$ are positive constant parameters. By introducing this weighting function, temperature-tracking errors at desired locations are specially penalized such that close tracking is enforced at these locations. This helps to improve the tracking performance when the approximated melting interface is not well designed, with strict physical feasibility.

Remark 1: In the above control inputs optimization problem, the laser power u and the scanning speed v are two control inputs to be optimized. As reported in [17, 22], the height of the deposited layer is mainly controlled by $\frac{\dot{m}_P}{v}$, namely the amount of new powder material delivered per unit length on the track. Therefore, in this paper, the powder feed rate $\dot{m}_P$ is considered as a dependent variable that is adjusted with respect to the scanning speed v to ensure a desired deposition height H. Moreover, with the desired deposition height and the back and front radii, the liquid-gas interface is assumed sufficiently approximated by Eq. (1). Negligible errors were found from proceeding with this assumption and therefore we will not include this interface in the optimization discussions.

Derived Adjoint Equations

Analogous to their counterparts with ODE constraints, the optimization problems involving PDE constraints are often solved using gradient-based methods such as the steepest descent method. In this paper, we apply the adjoint-based sensitivity method by using the Lagrangian formalism [23]. By applying the first order optimality conditions, also known as the Karush-Kuhn-Tucker (KKT) conditions [23] on the Lagrangian function, the following adjoint system of equations can be derived:

$$\rho_S C_S \nabla \cdot (v p_S) - k_S \nabla^2 p_S = 0 \qquad \text{in } \Omega_S \quad (6.1)$$

$$\rho_L C_L \nabla \cdot (v p_L) - k_L^* \nabla^2 p_L = 0 \qquad \text{in } \Omega_L \quad (6.2)$$

$$k_S \frac{\partial p_S}{\partial \mathbf{n}} - \rho_S C_S (p_S v \cdot \mathbf{n}) = 0 \qquad \text{on } \Gamma_{SG} \quad (6.3)$$

$$k_L^* \frac{\partial p_l}{\partial \mathbf{n}} - \rho_L C_L (p_L v \cdot \mathbf{n}) = 0 \qquad \text{on } \Gamma_{LG} \quad (6.4)$$

$$p_S = 0 \qquad \text{on } \Gamma_S \quad (6.5)$$

$$\left[k \frac{\partial p}{\partial \mathbf{n}} - \rho C (p v \cdot \mathbf{n})\right]_L^S + \alpha_1 w(x) \left(\frac{T - T_m}{{T_m}^2}\right) = 0 \qquad \text{on } \Gamma_{SL} \quad (6.6)$$

where the variables p_S and p_L are the adjoint variables in the solid and liquid domains, respectively and p_{SL} is that for the melting interface.

The gradient equations for the control variables u and v can be obtained similarly:

$$\nabla_u = \int_{\Gamma_{SG}} (p_S * \alpha_{att}) + \int_{\Gamma_{LG}} (p_L * \alpha_{att}) = 0 \quad (7.1)$$

$$\nabla_v = \int_{\Omega_S} \rho_S C_s \frac{\partial T_S}{\partial x} p_S + \int_{\Omega_L} \rho_L C_L \frac{\partial T_L}{\partial x} p_L + \int_{\Gamma_{SL}} \rho_L L n_x \cdot \mathbf{n} p = 0 \qquad (7.2)$$

where n_x is the unit vector in x direction. Detailed derivations of the above adjoint and gradient equations are provided in [21].

Computational Algorithm

We propose the following algorithm to calculate the solution of the optimization problem using the adjoint and gradient equations listed above. Similar to the compact notation used in Eq. (4.2) for the system equations, the notation $p = \mathrm{Adj}(T, v)$ will be used to represent the adjoint equations compactly.

Algorithm 1: Adjoint-Based Gradient Method

Input: Initial values u_0, v_0

Output: Optimized control inputs $\hat{u}^*$, $\hat{v}^*$ and the corresponding temperature $\hat{T}^*$, objective function $\hat{J}^*$

Initialize: $\hat{T} = \mathrm{Sys}(u_0, v_0)$, $\hat{p} = \mathrm{Adj}(\hat{T}, v_0)$, $\hat{J} = J(u_0, v_0)$

While $\hat{J} - \tilde{J} > \varepsilon$

$\hat{J} \leftarrow \tilde{J}$, $\hat{u} \leftarrow \tilde{u}$, $\hat{v} \leftarrow \tilde{v}$, $\hat{p} \leftarrow \tilde{p}$

Search direction for u: $n_u = \mathrm{sgn}[\nabla_u(\hat{p})]$

Search step size for u: $\delta_u := \arg\min_{\delta_u} J(\tilde{u}, \hat{v})$ with $\tilde{u} = \hat{u} - n_u * \delta_u$

$\tilde{T} = \mathrm{Sys}(\tilde{u}, \hat{v})$, $\tilde{p} = \mathrm{Adj}(\tilde{T}, \hat{v})$, $\tilde{J} = J(\tilde{u}, \hat{v})$

Search direction for v: $n_v = \mathrm{sgn}[\nabla_v(\tilde{T}, \tilde{p})]$

Search step size for v: $\delta_v := \arg\min_{\delta_v} J(\tilde{u}, \tilde{v})$ with $\tilde{v} = \hat{v} - n_v * \delta_v$

$\tilde{T} = \mathrm{Sys}(\tilde{u}, \tilde{v})$, $\tilde{p} = \mathrm{Adj}(\tilde{T}, \tilde{v})$, $\tilde{J} = J(\tilde{u}, \tilde{v})$

End while

$\hat{u}^* = \tilde{u}$, $\hat{v}^* = \tilde{v}$, $\hat{J}^* = \tilde{J}$, $\hat{T}^* = \tilde{T}$

In the above algorithm, ε denotes the desired convergence margin for the algorithm.

Remark 2: The computational algorithm proposed above proceeds sequentially first on the control variable u, and then on v. This is based on the observation that the search direction for laser power u is only determined by the adjoint variable p, which is directly affected by $T - T_m$ as an input into the adjoint system (see Eq. (6.6)). Thus, it is reasonable to expect that the objective function is more sensitive to laser power and start the search with this variable.

Case Study – Laser Cladding Process

To validate the proposed optimal control scheme, the laser cladding process is considered here as an example. In this process, a thin coating (cladding layer) is deposited on a metal substrate to provide superior wear and corrosion resistance. An Nd:YAG laser with the wavelength of 1.06 μm is used as a heat source to deposit powder particles onto a steel substrate.

The anisotropic enhanced thermal conductivity model, with an enhancement factor of 2, is applied in the liquid domain in laser moving direction [10]. Major material properties [7] and the process design parameters used in the simulation case study can be found in [21].

The objective in this process is to achieve the desired melting surface geometry denoted by back/front radii and melting pool depth with optimal combinations of laser power and scanning speed. To implement the computational algorithm, COMSOL Multiphysics and Matlab are used jointly. Both the system and the derived adjoint PDEs are solved using COMSOL while the main optimization algorithm is implemented in Matlab. The simulation results are demonstrated in Figs. 3-5.

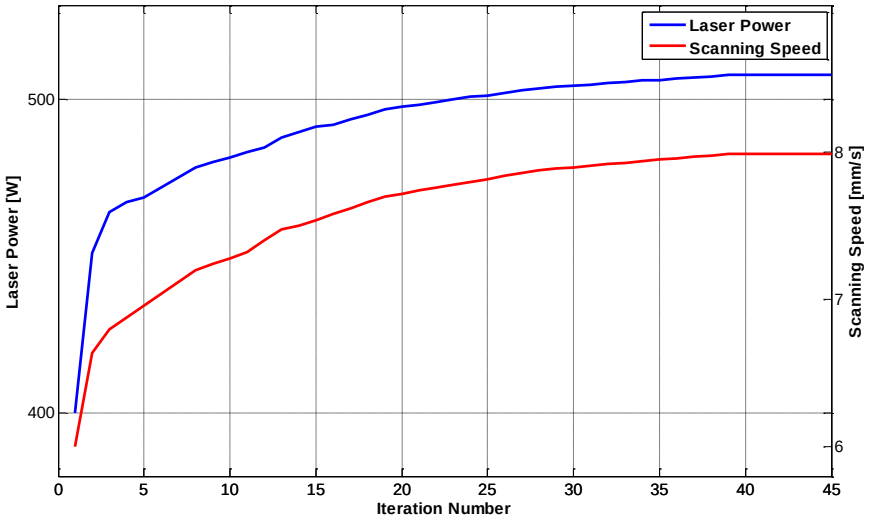

Fig. 3 Evolution of laser power and scanning speed in weighted optimization

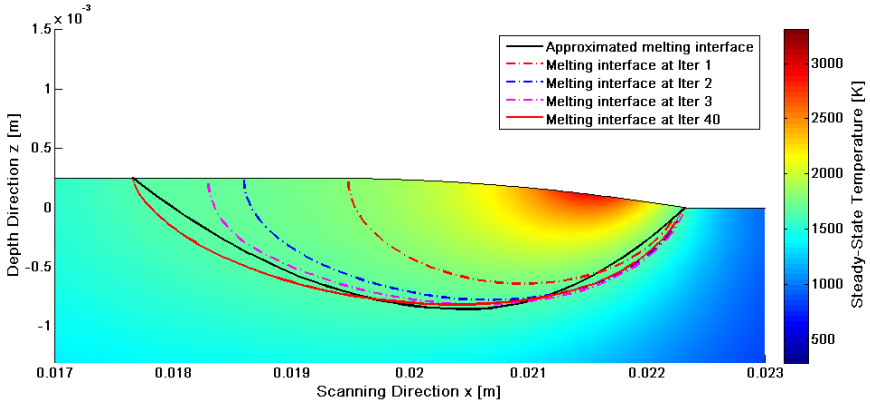

Fig. 4 Evolution of melting interface in weighted optimization

Fig. 3 and Fig. 4 illustrate the evolution of control inputs and the melting interface geometry in the optimization with the weighting function. The weighting function parameters are selected to be: $\alpha_2 = 300, \alpha_3 = 200, \alpha_4 = 500$. As the computational algorithm proceeds, the control inputs approach their optimal values, which are $\mathrm{u} = 507.8\,\mathrm{W}$ and $\mathrm{v} = 8.0\,\mathrm{mm/s}$ respectively. Similarly in Fig. 4, starting from an initial guess that generates the actual melting

interface far away from the desired one, the proposed optimal control algorithm is able to drive the melting interface close to the desired one. The tracking performance in terms of error percentage of process target parameters is analyzed in Table 1 and will be discussed below.

A similar simulation without the weighting function was also conducted under the same condition and the comparison of the optimized melting interface is demonstrated in Fig. 5.

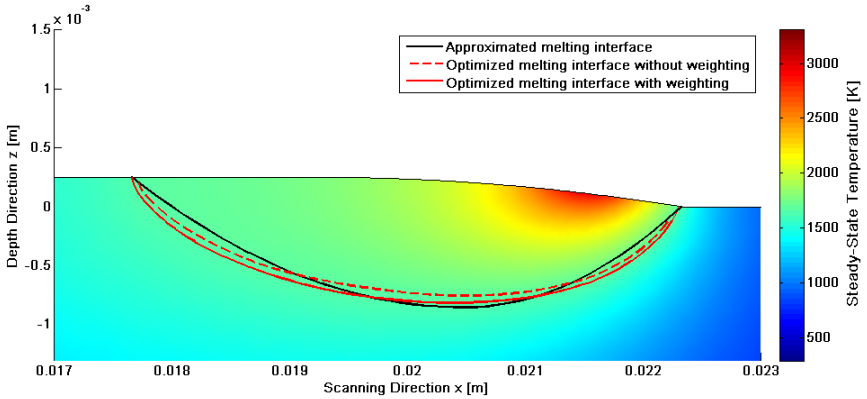

Fig. 5 Comparison of melting interfaces in optimization

As we can see from Fig. 5, with the optimized control inputs $u = 510.9\,W$ and $v = 8.5\,mm/s$ in this case, the actual melting interface tends to be shallower than that with the weighting function. This leads to degraded tracking of the melting pool depth. Comparison of the tracking performance in these two simulation studies is provided in Table 1.

		Optimization without weighting function	Optimization with weighting function
Tracking error percentage	Laser power [W]	510.9	507.8
	Scanning speed [mm/s]	8.5	8.0
	Back radius r_b [%]	1.2	0.3
	Front radius r_f [%]	15.2	10.9
	Penetration depth D [%]	11.5	4.6

Table 1 Comparison of optimizations with and without weighting function

From the above table, we can see that with the weighting function in optimization, tracking performance in terms of error percentage of process target parameters r_b, r_f and D are improved. This illustrates the usefulness of the weighting scheme towards improved tracking performance for those target parameters. Moreover, it is worth noting that a relatively large tracking error appears in the front radius; this is because as the laser source moves, the front radius is much shorter than the back radius in the melting pool, leading to a much larger

temperature gradient in the front. Therefore, temperature tracking error can be expected to be higher in this area. Moreover, considering the fact that the temperature in the melting pool is usually very high (as shown in Fig. 4) and there exists a *mushy* zone where solid and liquid phases co-exist with temperatures close to the melting temperature, the remaining error percentage obtained by the optimization algorithm may be taken as satisfactory for tracking the desired process parameters.

Conclusion

This paper proposes a multivariable control inputs optimization scheme for melting interface tracking in LAPD processes. The intermediate segments of these processes are considered where steady state can be assumed in a moving coordinate system. Then, by approximating the geometry of the free interfaces from desired process target parameters, the control problem can be formulated as one of closely tracking a pre-specified melting interface with optimal control inputs in fixed domains. The resulting multivariable PDE-constrained optimization problem is solved by the adjoint-based gradient method. A computation algorithm is also offered for obtaining the optimal inputs. The proposed optimization scheme has been illustrated for a laser cladding process as a typical example of LAPD processes. To achieve improved tracking performance, a weighting scheme is also included in the objective function. Simulation based illustrations on a laser cladding process demonstrated the effectiveness of the proposed approaches.

Furthermore, we note that the proposed control scheme only deals with the steady state segments and servers as a starting open-loop solution for the control of LAPD processes. Research efforts are still needed to incorporate closed-loop controls to accommodate variable deposition geometries as well as exogenous disturbances in these processes.

Acknowledgment

The authors acknowledge the financial support received for this research, in part, from the US National Science Foundation under NSF Grant No. CMMI-1055254 and the U.S. Department of Energy (DOE) Graduate Automotive Technology Education Program under grant No. DE-EE0005571.

References

[1] Saldi, Z. S., "Marangoni driven free surface flows in liquid weld pools," Ph.D. thesis, Delft University of Technology, Delft, Netherlands., 2012.
[2] Morville, S., Carin, M., Peyre, P., Gharbi, M., Carron, D., Le Masson, P., and Fabbro, R., "2D longitudinal modeling of heat transfer and fluid flow during multilayered direct laser metal deposition process," Journal of Laser Applications, 24, p. 032008, 2012.
[3] Traidia, A., "Multiphysics modelling and numerical simulation of GTA weld pools," Ph. D. thesis, Ecole Polytechnique, Palaiseau, France, 2011.
[4] Sethian, J., and Smereka, P., "Level set methods for fluid interfaces," Annual Review of Fluid Mechanics, 35(1), pp. 341-372, 2003.
[5] Pinkerton, A. J., and Lin, L., "Modelling powder concentration distribution from a coaxial deposition nozzle for laser-based rapid tooling," Journal of manufacturing science and engineering, 126(1), pp. 33-41, 2004.

[6] Wen, S., and Shin, Y. C., "Modeling of transport phenomena during the coaxial laser direct deposition process," Journal of Applied Physics, 108, 044908, 2010.
[7] Qi, H., Mazumder, J., and Ki, H., "Numerical simulation of heat transfer and fluid flow in coaxial laser cladding process for direct metal deposition," Journal of applied physics, 100, 024903, 2006.
[8] Han, L., and Liou, F., "Numerical investigation of the influence of laser beam mode on melt pool," International journal of heat and mass transfer, 47(19), pp. 4385-4402, 2004.
[9] Safdar, S., Pinkerton, A. J., Li, L., Sheikh, M. A., and Withers, P. J., "An anisotropic enhanced thermal conductivity approach for modelling laser melt pools for Ni-base super alloys," Applied mathematical modelling, 37(3), pp. 1187-1195, 2013.
[10] Kamara, A., Wang, W., Marimuthu, S., and Li, L., "Modelling of the melt pool geometry in the laser deposition of nickel alloys using the anisotropic enhanced thermal conductivity approach," Proceedings of the Institution of Mechanical Engineers, Part B: Journal of Engineering Manufacture, 225(1), pp. 87-99, 2011.
[11] Bernauer, M. K., and Herzog, R., "Optimal control of the classical two-phase Stefan problem in level set formulation," SIAM Journal on Scientific Computing, 33(1), pp. 342-363, 2011.
[12] Volkov, O., and Protas, B., "An inverse model for a free-boundary problem with a contact line: Steady case," Journal of Computational Physics, 228(13), pp. 4893-4910, 2009.
[13] Hinze, M., and Ziegenbalg, S., "Optimal control of the free boundary in a two-phase Stefan problem," Journal of Computational Physics, 223(2), pp. 657-684, 2007.
[14] Vossen, G., and Hermanns, T., "On an optimal control problem in laser cutting with mixed finite-/infinite-dimensional constraints," Journal of Industrial and Management Optimization, 10(2), pp. 503-519, 2014.
[15] Vossen, G., Hermanns, T., and Schüttler, J., "Analysis and optimal control for free melt flow boundaries in laser cutting with distributed radiation," ZAMM-Journal of Applied Mathematics and Mechanics/Zeitschrift für Angewandte Mathematik und Mechanik, 2013.
[16] Volkov, O., Protas, B., Liao, W., and Glander, D. W., "Adjoint-based optimization of thermo-fluid phenomena in welding processes," Journal of Engineering Mathematics, 65(3), pp. 201-220, 2009.
[17] Fathi, A., Khajepour, A., Toyserkani, E., and Durali, M., "Clad height control in laser solid freeform fabrication using a feedforward PID controller," The International Journal of Advanced Manufacturing Technology, 35(3-4), pp. 280-292, 2007.
[18] Toyserkani, E., Khajepour, A., and Corbin, S., "3-D finite element modeling of laser cladding by powder injection: effects of laser pulse shaping on the process," Optics and Lasers in Engineering, 41(6), pp. 849-867, 2004.
[19] Song, L., and Mazumder, J., "Feedback control of melt pool temperature during laser cladding process," Control Systems Technology, IEEE Transactions on, 19(6), pp. 1349-1356, 2011.
[20] Hofman, J., Pathiraj, B., van Dijk, J., de Lange, D., and Meijer, J., "A camera based feedback control strategy for the laser cladding process," Journal of Materials Processing Technology, 2012.
[21] Cao, X., and Ayalew, B., "PDE-based Multivariable Control Input Optimization for Laser-Aided Powder Deposition Processes," Journal of Manufacturing Science and Engineering, under reivew, 2014.
[22] De Oliveira, U., Ocelik, V., and De Hosson, J. T. M., "Analysis of coaxial laser cladding processing conditions," Surface and Coatings Technology, 197(2), pp. 127-136, 2005.
[23] Tröltzsch, F., Optimal control of partial differential equations: theory, methods, and applications, American Mathematical Soc., 2010.